Characterization of isotropic solids with nonlinear surface acoustic wave pulses

Al. A. Kolomenskii and H. A. Schuessler
Texas A&M University, Department of Physics, College Station, Texas 77843-4242
(Received 9 October 2000; published 6 February 2001)

The nonlinear propagation of high-amplitude surface acoustic wave (SAW) pulses in two isotropic materials, polycrystalline aluminum and synthetic fused silica, was studied and exhibited qualitatively different types of nonlinear behavior. A single SAW pulse excited by a nanosecond laser pulse through a strongly absorbing layer was detected at two probe spots along the propagation path with a dual-probe-beam deflection setup. In this way the nonlinear changes of the SAW pulse shape were observed. For aluminum, the compression of the SAW pulse and formation of one negative (inward the solid) narrow peak in the registered normal surface velocity and a shock front in the in-plane velocity were detected. This nonlinear behavior corresponds to a positive value of the nonlinear acoustic constant responsible for the local nonlinearity. For fused silica, the temporal extension of the SAW pulse and formation of two positive sharp peaks in the normal velocity related to two shock fronts in the in-plane velocity were registered. In this case the acoustic constant of the local nonlinearity is negative. The nonlinear acoustic constants for each material were evaluated by fitting the theoretical model based on the nonlinear evolution equation to the registered SAW pulses. The values obtained were found to be consistent with those calculated from nonlinear elastic moduli of the third order, measured previously with different techniques for similar materials. The characterization of solids by their nonlinear acoustic and elastic constants promises to be complimentary and more specific than the characterization based on the linear properties.

DOI: 10.1103/PhysRevB.63.085413 PACS number(s): 62.65.+k, 43.25.+y, 62.20.−x

I. INTRODUCTION

Studies of nonlinear properties of surface acoustic waves (SAW's) recently attracted substantial interest in different fields.[1] Nonlinear characteristics of solid materials set the limit for achieving high signal-to-noise ratios in many ''linear'' applications including acousto-electronic delay lines, filters, and sensors. Some devices for signal processing, such as convolvers and correlators, just utilize nonlinearity for their functioning. In seismology, nonlinear processes can play an essential role in the propagation of seismic waves generated by earthquakes.[2] Changes in the profile of high-amplitude SAW's can strongly affect their interaction with mechanical particles residing at the surface, and can be used for enhancing the surface cleaning effect.[3] In materials science, studies of the nonlinear behavior of SAW's provide data for the determination of nonlinear elastic and acoustic constants.[4] These constants can be used in a novel approach for materials characterization, in particular under conditions of strong dynamic loading. The observation of nonlinearity in SAW's is facilitated by their localization in a layer near the surface with about one wavelength depth.

In earlier related experiments the generation of higher harmonics in SAW's was observed with interdigital transducers,[5,6] but only recently first observations of strongly nonlinear SAW pulses with formation of shock fronts were performed with laser generation and detection techniques.[4,7] The correct theoretical description of nonlinear SAW's has been a long-standing problem. Two comprehensive models were developed recently for the description of nonlinear SAW pulses: one model employs a Hamiltonian formalism,[8] and the other model describes the surface velocities in SAW's with an evolution equation.[9] The approach based on the evolution equation gives a consistent description of nonlinear SAW's without any *a priori* assumptions on the decay of the velocity into the depth of the solid. In addition, this approach permits a rather simple interpretation of the results using three nonlinear acoustic constants. Therefore it will be used in our consideration.

In this work we used laser-generated high-amplitude SAW pulses to study nonlinear properties of two isotropic materials: polycrystalline aluminum and synthetic fused silica, demonstrating in this way the versatility of the method and its applicability to studies of different classes of solids. We have shown that these two materials possess different signs of the acoustic constant responsible for the local nonlinear distortions and therefore high-amplitude SAW pulses exhibit in them two qualitatively different types of nonlinear behavior.

II. EXPERIMENTAL ARRANGEMENT

In the present study, a *Q*-switched Nd:yttrium aluminum garnet (YAG) laser with a pulse energy of up to 100 mJ, duration of 26 ns and optical wavelength of 1.06 μm was employed as the excitation laser (EL in Fig. 1). Samples of polycrystalline aluminum (an alloy with 97.9% Al, 0.6% Si, 0.28% Cu, 1% Mg, 0.2% Cr) had lateral dimensions of $76 \times 76\,\mathrm{mm}^2$ and a thickness of 4 mm, which was sufficient for observation of the pure surface Rayleigh mode for all high frequencies of interest (>1 MHz). The dimensions of the synthetic fused silica samples (Suprasil 1) were $40 \times 40 \times 3.5\,\mathrm{mm}$. For the generation of SAW's with a plane front, the laser pulse was sharply focused with a cylindrical lens CL to a strip with a length ~ 10 mm and a width ~ 10 μm. The energy of the laser pulse was high enough to cause optical breakdown at the surface of both fused silica and aluminum, which was accompanied by an audible response.

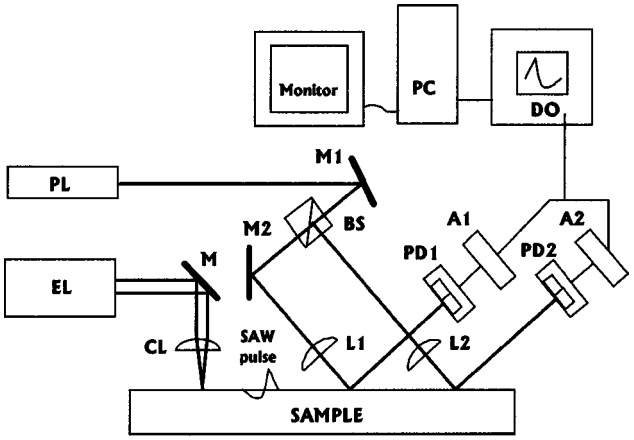

FIG. 1. Schematic outline of the experimental setup.

However, the generation mechanism associated with optical breakdown could not provide sufficient amplitudes for the observation of nonlinear SAW pulses, since the efficiency of the generation process was strongly reduced by the screening of the laser radiation by the plasma formed in the ionized vapor. In order to maximize the conversion of the laser pulse energy into mechanical energy, a thin (about 100 μm) strongly absorbing a layer of carbon suspension in water was deposited before the excitation in the area of the laser irradiation spot on the surface. For efficient generation the thickness of the carbon layer was made larger than the penetration depth of the laser radiation into the layer.

The dual-probe-beam-deflection technique[4] was used for the detection of nonlinear SAW's. This technique provided the possibility to register the nonlinear transformation of SAW pulses in a single laser shot, which is important to avoid errors connected with variations of the output energy of the pump laser.

In the detection setup, the initial beam of the probe laser PL (Spectra Physics cw diode-pumped solid-state laser ''Millenia'' with an output power of up to 5 W) was split into two subbeams by the beam splitter BS. The subbeams were focused onto the sample surface with the gradient-index lenses L1, L2 to form two probe spots of about 8 μm size. This allowed us to probe the SAW pulse shape with nanosecond resolution in a small portion of the wave front. The registration was performed in the far wave field several millimeters away from the source, so that all transient processes of the generation were excluded.

After reflection from the sample surface each of the subbeams was split and detected by a pair of photodiodes (PD1 and PD2, respectively). The outputs of the photodiodes in each pair were connected differentially, thus providing a signal proportional to the angular shift of the subbeam. This shift is determined by a change of the surface inclination within the probe spot. When a SAW pulse is passing through the probe spot the surface inclination is proportional to the normal component of the surface velocity. For an absolute measurement of the normal surface velocity the detection setup was calibrated before each laser shot. For this purpose a signal was registered for an artificially created surface inclination of known magnitude.

The level of the probe laser power was chosen according to the reflectivity of the sample. It was set high enough (200 mW for aluminum and about 1 W for fused silica) to compensate for the decrease of the laser power due to the losses on the mirrors, the surface of the sample, and in the beam splitter, so that sufficient signal-to-noise ratio (typically about 20) could be obtained. The upper limit for the power of the probe beam was set to avoid the melting of the sample surface and saturation of the photodiodes. The SAW pulse signal was registered in a wide frequency range with a digital oscilloscope (Tektronix TDS 680 C, 1 GHz real-time bandwidth).

III. THEORETICAL MODEL

The deposition of the laser pulse energy in the thin absorption layer and subsequent thermalization produce an increase of pressure and a strong pulse in the normal force acting on the surface of the solid. The focusing of the laser beam in a narrow strip creates a line-shaped source, which can be modeled as a pressure pulse $p(\mathbf{r},t)$ with a Gaussian spatial and temporal distribution $p(\mathbf{r},t)=p_0\exp[-x^2/a^2-t^2/\tau_0^2]$, where a and τ_0 are the characteristic source dimension and duration of the pulse. Since the pressure impact is still small in comparison to the elastic moduli of the solid, a linear approximation can be used to evaluate the SAW pulse in the wave field close to the source. The normal component of the surface velocity can be described by the expression[10]

$$v(\mathbf{r},t)=\frac{c_R}{4}\frac{ac_R\tau_0}{b^2}\frac{p_0}{\rho c_t^2}\Gamma\gamma\int_0^\infty k\exp(-k^2/4)\cos(k\xi)dk. \tag{1}$$

Here $b=(a^2+c_R^2\tau_0^2)^{1/2}$ is the characteristic wavelength of the SAW pulse, and the dimensionless combinations of the elastic constants can be presented in the form

$$\gamma=[(1-\delta/\delta_1)/(1-\delta)]^{1/4},$$
$$\Gamma=\{(1-\delta/2)[(1-\delta)^{-1}+(\delta_1-\delta)^{-1}]-2\}^{-1}, \tag{2}$$

where $\delta=c_R^2/c_t^2$, $\delta_1=c_l^2/c_t^2$, and $c_{t,l,R}$ are the propagation velocities of the transversal and longitudinal bulk acoustic waves and surface Rayleigh waves. For aluminum the values consistent with our measurements and used for calculations are $c_l=6.42\times10^5$ cm/s, $c_t=3.11\times10^5$ cm/s, $c_R=2.91\times10^5$ cm/s, $\gamma=1.58$, $\Gamma=0.38$, $\rho=2.70$ g/cm^3, and for fused silica $c_l=5.94\times10^5$ cm/s, $c_t=3.79\times10^5$ cm/s, $c_R=3.42\times10^5$ cm/s, $\gamma=1.38$, $\Gamma=0.64$, $\rho=2.20$ g/cm^3.

The appearance of the acoustic nonlinearity is connected with the nonlinear elastic behavior of the solid material. The shape of the high-amplitude SAW pulse is changing as nonlinear distortions are accumulated with the propagation distance. This process can be described by an evolution equation.[9] Taking into account attenuation, which becomes especially important with the nonlinear steepening of the wave fronts, the evolution equation for the tangential component of the surface velocity v in the case of SAW's with a plane front can be presented in the form

$$c_R^2\frac{\partial v}{\partial x}=\varepsilon_1 v\frac{\partial v}{\partial \tau}+\frac{\varepsilon_2}{2}\frac{\partial}{\partial \tau}\{v^2+(H[v])^2\}+\varepsilon_3\left\{v\frac{\partial v}{\partial \tau}+H\left[vH\left[\frac{\partial v}{\partial \tau}\right]\right]\right\}+\beta\frac{\partial^2 v}{\partial \tau^2}. \quad (3)$$

Here $\tau=t-x/c_R$ is the retarded time. The nonlinear acoustic constants $\varepsilon_{1,2,3}$ include combinations of the shear and bulk moduli as well as the third-order nonlinear moduli of the solid.[11] $H[v]$ is the Hilbert transform operator [see Eq. (4)]. Equation (3) describes the changes in the wave profile (left-hand side) induced by the different effects presented by the terms on the right-hand side: dependence of the propagation velocity on the amplitude (this term is proportional to ε_1 and describes the local nonlinearity), nonlocal nonlinear interactions in the SAW (the terms containing ε_2 and ε_3), and absorption proportional to the attenuation parameter β.

The SAW amplitude can be conveniently characterized by the acoustic Mach number $M=v/c_R$, defined as the ratio of the peak in-plane surface velocity to the propagation velocity of the SAW. It is equal in order of magnitude to the relative deformation of the material and to the surface inclination produced by the SAW. For the observation of nonlinear acoustic effects, the acoustic Mach number should be sufficiently large; however, numerically it still remains a small parameter.

It should be noted that the normal component of the surface velocity v_n as a function of the retarded time can be calculated from the in-plane component and visa versa using the Hilbert transform operator

$$v=\frac{1}{\gamma}H[v_n],\quad v_n=-\gamma H[v],\qquad H[v]=\frac{1}{\pi}\mathrm{P}\int_{-\infty}^{+\infty}\frac{v(t')dt'}{t'-t}. \quad (4)$$

The constant γ is defined in Eq. (2).

Equations (3) and (4) were solved numerically using their Fourier transform representations.[9] To limit high frequencies at shock fronts a small artificial attenuation with $\beta\sim 3\times10^{-8}$ cm was introduced. The shape of the SAW pulse at the second registration spot was calculated from the waveform measured at the first registration spot. Thus, for the determination of the nonlinear acoustic constants the SAW pulse shape itself at the first distance is not important, since these constants are extracted from the *change* of the pulse shape during the nonlinear propagation.

IV. RESULTS

The linear SAW pulse excited in aluminum and registered at a distance of $x_1=16$ mm from the source is shown in Fig. 2. The amplitude of the pulse, is relatively small in this case (the corresponding Mach number is about 10^{-3}). In Figs. 3(a) and 3(b) the waveforms of a SAW pulse with a much higher amplitude (Mach number is about 5×10^{-3}) detected at two distances from the source $x_1=13.9$ mm and $x_2=26.7$ mm are shown. As follows from comparison with the calculated waveform of Fig. 2, for the generation of such a high-amplitude pulse a pressure of ~3 GPa should have been reached in the excitation region. The first waveform, measured at the smaller distance, has a duration of 70 ns [full width at half maximum (FWHM)] while the second waveform measured at the larger distance has a duration of 45 ns. Thus, in aluminum the nonlinearity caused temporal compression of the central high-amplitude part of the SAW pulse during propagation. At the second distance, the negative peak becomes narrower; however, the two wings of the pulse decay slower from the center of the pulse. This means that simultaneously with frequency up-conversion processes also down-conversion takes place.

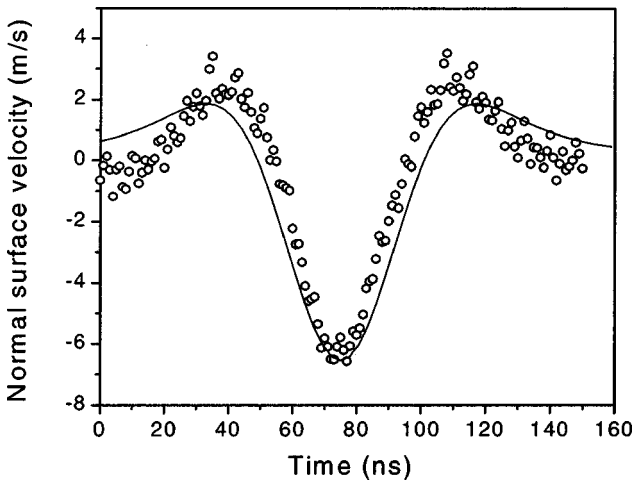

FIG. 2. SAW pulse of relatively small amplitude (''linear pulse'') registered in aluminum at a distance $x=13.9$ mm. Open circles, experimental points; solid line, calculation according to Eq. (1) with $p_0=0.55$ GPa.

The corresponding in-plane components of the surface velocity for the pulses of Figs. 3(a) and 3(b) were calculated with the Hilbert transform and are shown in Figs. 4(a) and 4(b). The time interval between the peaks of the negative and positive polarity in the in-plane velocity component decreases with propagation distance. This means that the part of the pulse with negative polarity moves slower than the part of the pulse with positive polarity. As a result, one shock front is formed in the center of the pulse. This shock front corresponds to a sharp negative peak in the normal surface velocity [see Fig. 3(a)]. The amplitude of the in-plane surface velocity in our experiments with aluminum was about 13 m/s and corresponded to a Mach number of ~0.005.

Solid lines in Fig. 3(b) and Fig. 4(b) show the pulse calculated with Eqs. (3) and (4) at the second distance, when the first observed waveform was used as the initial profile in the calculation. The waveforms plotted were obtained by varying two nonlinear acoustic constants ε_1 and ε_3, and fitting the calculated waveform of the normal surface velocity at the second distance to the experimentally observed one. The constant ε_2 depends only on the second-order elastic constants according to the explicit expressions for this constant[11] and is determined with an accuracy ~1%; therefore its value was fixed in the calculation as $\varepsilon_2=-1.02$.

In Fig. 5 waveforms of SAW pulses observed in fused

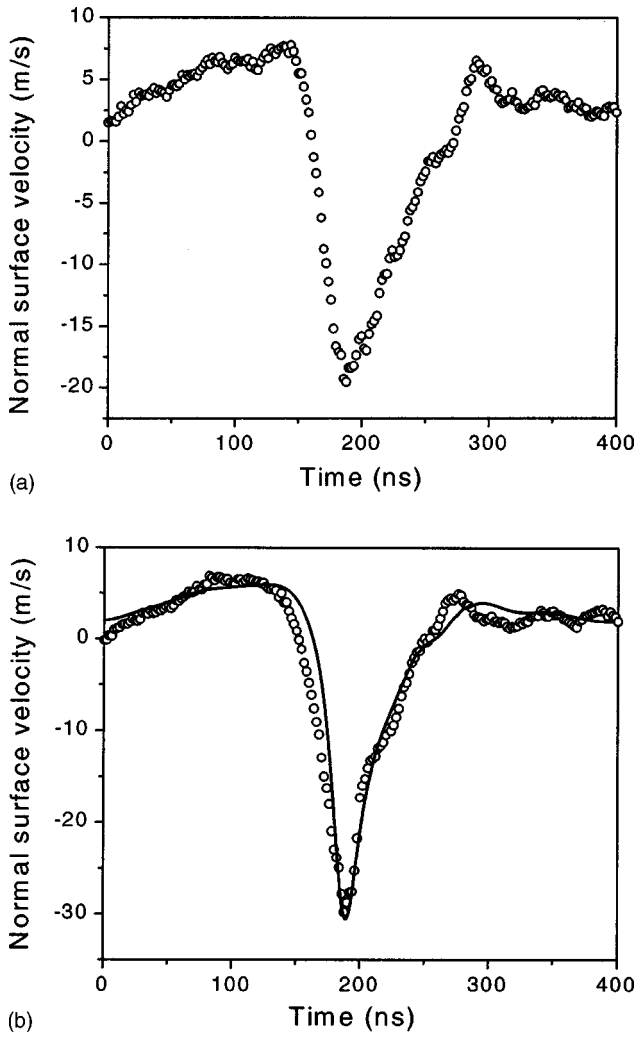

FIG. 3. Normal surface velocity of the nonlinear SAW pulse measured in aluminum at distances (a) $x_1 = 13.9$ mm and (b) $x_2 = 26.7$ mm from the source. Open circles, experimental points; solid line, calculation with the evolution equation (2).

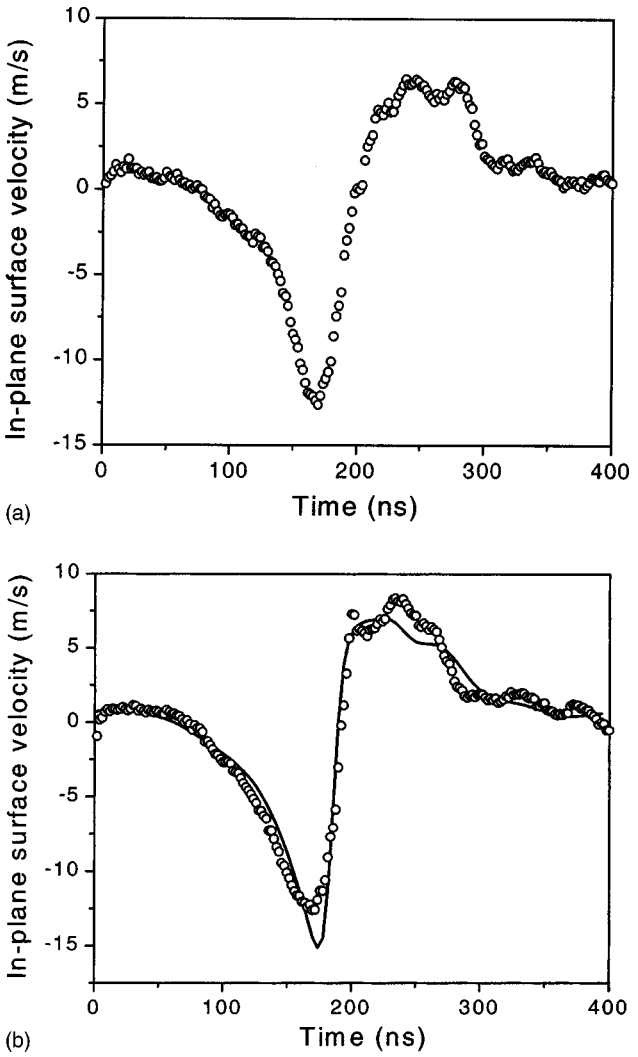

FIG. 4. In-plane surface velocity corresponding to the waveforms of Figs. 3(a) and 3(b) measured in aluminum at distances (a) $x_1 = 13.9$ mm and (b) $x_2 = 26.7$ mm from the source. Open circles, calculation with the Hilbert transform using experimental points; solid line, calculation with the evolution equation (2).

silica are shown. The waveform at the first distance has the duration of the positive peaks about equal to that of the negative phase of the pulse. With an increase of the propagation distance the positive peaks acquire higher amplitudes and become narrower, the duration of the central negative part of the pulse increases leading to an increase of the whole duration of the pulse. At large distances the waveform tends to acquire an universal shape with two narrow positive peaks separated by a valley. The solid line presents the result of the calculation with Eqs. (3) and (4), open circles show experimental points.

When the SAW pulse had an amplitude slightly above the one shown in Fig. 5, the formation of small cracks on the pulse track was observed in fused silica at distances 5–10 mm from the source. The shape of the pulse was more distorted in this case. The cracks observed may result from the formation of shock fronts, when the stress in the material exceeds the limit of fracture.

The corresponding in-plane components of the surface velocity for the pulses of Figs. 5(a) and 5(b) are shown in Figs. 6(a) and 6(b). At the larger propagation distance ($x_2 = 15.72$ mm) two clearly seen shock fronts are formed. These shock fronts correspond to the observed peaks in the normal surface velocity. The shock front formed in the head of the pulse propagates with lower velocity than the shock front formed in the tail. The difference in their velocities is ~ 16 m/s, or 0.5% of c_R. This difference is responsible for the observed increase of the pulse duration. The amplitude of the in-plane surface velocity at the first distance consists ~ 20 m/s and corresponds to a Mach number ~ 0.006.

The calculations revealed that the same absolute changes in three nonlinear acoustic constants cause different mean square deviations of the calculated and experimental waveforms. For comparison, a change of 0.1 from the optimal values provided relative deviation of 30% for ε_1, 8% for ε_2, and 6% for ε_3. Thus, the accuracy of the evaluation of these constants was higher for ε_1 and less for ε_2 and ε_3. However, as ε_2 depends only on the elastic moduli of the second order,

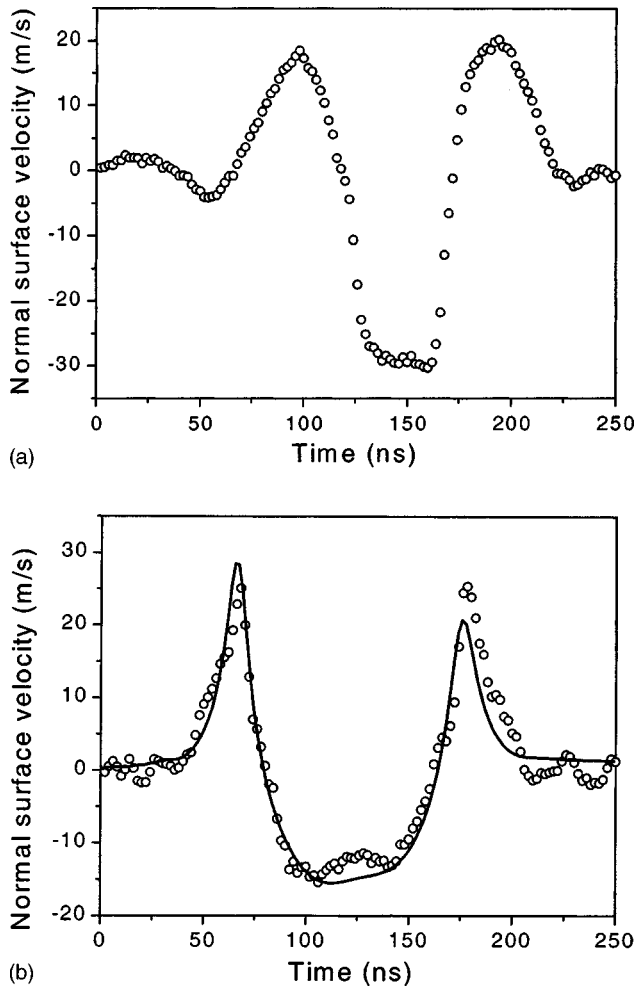

FIG. 5. Normal surface velocity of the nonlinear SAW pulse measured in fused silica at two distances: (a) $x_1 = 4.6$ mm and (b) $x_2 = 15.7$ mm from the source. Open circles, experimental points; solid line, calculation with the evolution equation (2).

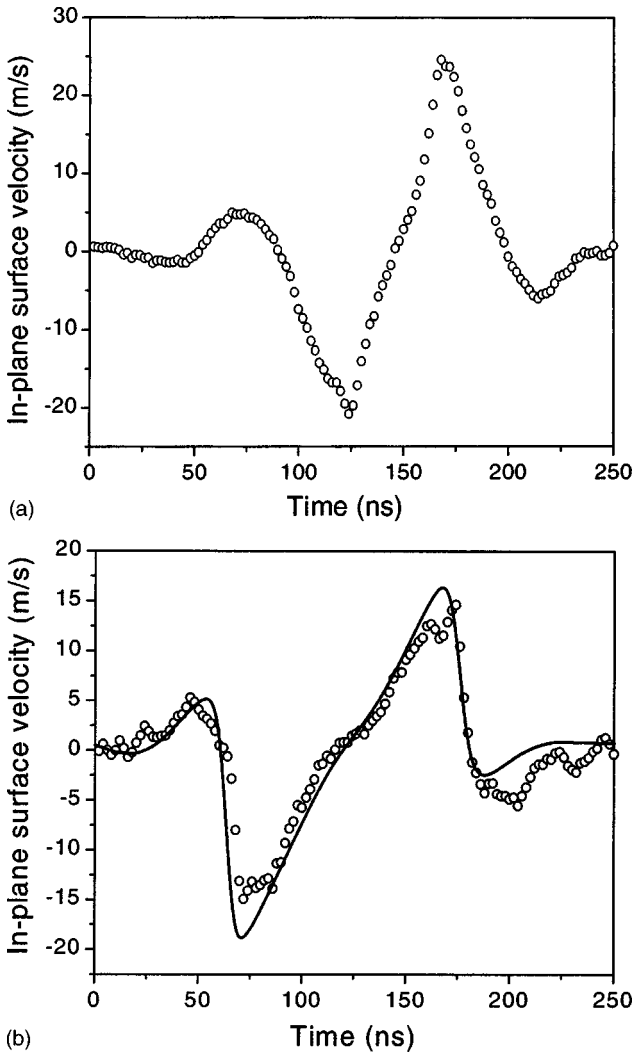

FIG. 6. In-plane surface velocity corresponding to the waveforms of Figs. 5(a) and 5(b) measured in fused silica. Open circles, calculation with the Hilbert transform using experimental points; solid line, calculation with the evolution equation (2).

its value was fixed and only two constants ε_1 and ε_3 were varied in the fitting procedure.

The procedure of the constant evaluation was repeated with five pairs of measured pulses for each material. For aluminum the following set of nonlinear acoustic constants was determined: $\varepsilon_1 = 0.7 \pm 0.1$, $\varepsilon_2 = -1.02 \pm 0.01$, and $\varepsilon_3 = 2.5 \pm 0.5$. For fused silica the evaluation yielded $\varepsilon_1 = -0.8 \pm 0.1$, $\varepsilon_2 = -0.25 \pm 0.005$, and $\varepsilon_3 = -4 \pm 0.5$.

V. DISCUSSION

Our results demonstrate that with an increase of the SAW pulse amplitude changes in the pulse shape due to nonlinearity take place. It follows from our calculations that variations of ε_1 (among three nonlinear constants) produce the largest effect on the nonlinear transformation of SAW pulses. Therefore we will refer to ε_1 as the main nonlinear constant.

For practical applications a rather important quantity is the length of the development of nonlinearity, or simply the nonlinear length. At this length the formation of a shock or an essential nonlinear distortion in the shape of the SAW pulse occurs. Since ε_1 induces the strongest effect on the nonlinear evolution of a SAW pulse, the nonlinear length can be estimated as $L \sim c_r \tau / 2\varepsilon_1 M$, where τ is the SAW pulse duration. For aluminum with $M = 0.005$ and $\tau = 70$ ns we find $L = 29$ mm, and for fused silica with $M = 0.006$ and $\tau = 60$ ns we find $L = 21$ mm. These estimates agree well with the observed shock front formation within distances of about 20 to 30 mm.

For aluminum, the parts of the pulse with higher in-plane velocity component propagate faster. This is in agreement with the positive value of the main nonlinear constant found for aluminum by fitting the theoretical model to the observed pulses.

In contrast, for fused silica the parts of the pulse with higher in-plane velocity component propagate slower. This conclusion complies with the negative value of the main nonlinear constant found for fused silica.

The nonlinear acoustic constants for polycrystalline aluminum alloys can be calculated from the data on second- and

third-order elastic moduli, determined from propagation velocities of ultrasonic waves in uniaxially stressed specimens.[12] For different alloys the calculated nonlinear constants varied within the limits $\varepsilon_1 = 0.83 - 1.01$, $\varepsilon_2 = (-0.84) - (-1.02)$, and $\varepsilon_3 = 2.86 - 5.95$. Thus, our results are consistent with these values, although for a more thorough comparison of values determined by different methods the measurements should be performed on samples with equal composition and properties.

The nonlinear acoustic constants for synthetic fused silica (Suprasil 1) determined in this work ($\varepsilon_1 = -0.8 \pm 0.1$ and $\varepsilon_3 = -4.0 \pm 0.5$) correlate well with the values $\varepsilon_1 = -0.84$ and $\varepsilon_3 = -4.2$, which we calculated from the third-order elastic moduli.[13] These moduli were determined for synthetic fused silica with the acoustic harmonic generation technique combined with ultrasonic beam mixing. We calculated also the nonlinear constants for fused quartz (Herasil) $\varepsilon_1 = -1.37$ and $\varepsilon_3 = -2.9$ from the third-order moduli, measured for this material with the hydrostatic compression and uniaxial loading method.[14] The values for $\varepsilon_{1,3}$ correlate better with the nonlinear acoustic constants $\varepsilon_1 = -1.0 \pm 0.3$ and $\varepsilon_3 = -2 \pm 1$ determined in Ref. 4 also for Herasil. These findings suggest that measurements with laser-generated nonlinear SAW pulses allow to register differences in the values of the nonlinear constants of fused quartz and synthetic fused silica. They reflect differences in manufacturing procedures resulting in different structures and physical properties. Indeed, fused quartz is formed from a melt of crushed crystalline quartz, whereas fused silica is produced by chemical combination of silicon and oxygen with flame hydrolysis or in a chemical vapor deposition process.[15] As a result, synthetic fused silica contains much less impurities and inhomogeneities, such as bubbles and striae, than fused quartz. It should be noted that the elastic moduli of the third order for synthetic fused silica and fused quartz[13,14] as well as nonlinear acoustic constants (ε_1 and ε_3) for these materials differ by at least 30%, whereas elastic moduli of the second order differ by only less than 1%. This comparison demonstrates that elastic moduli of the third order, which characterize the nonlinear elastic response of the material, are much more sensitive to the process of preparation and the structure of the material, than the elastic moduli of the second order corresponding to a linear response. Consequently, the measurements of nonlinear acoustic constants provide complimentary possibilities and some advantages for materials characterization.

VI. SUMMARY

Two qualitatively different types of nonlinear behavior of high-amplitude SAW pulses were observed, one in polycrystalline aluminum and the other in synthetic fused silica (Suprasil 1). The nonlinear acoustic constant of the local nonlinearity (ε_1) was found to be positive for aluminum. As a result, the compression of the SAW pulse and formation of one shock front in the in-plane surface velocity and a narrow negative (inward the solid) peak in the normal surface velocity were observed for this material. For fused silica the constant ε_1 was found to be negative and the temporal extension of the pulse was observed. In this case two shock fronts were formed in the leading part and the tail of the in-plane surface velocity. These shock fronts corresponded to two positive peaks in the normal surface velocity. The theoretical model of the propagation of the nonlinear SAW's in isotropic solids based on the evolution equation[9] allowed us to evaluate the nonlinear acoustic constants. For polycrystalline aluminum the values were $\varepsilon_1 = 0.7 \pm 0.1$, $\varepsilon_2 = -1.02 \pm 0.01$, and $\varepsilon_3 = 2.5 \pm 0.5$. These values are consistent with those that we calculated from previously measured third-order elastic moduli of aluminum alloys. For fused silica the set of constants evaluated was $\varepsilon_1 = -0.8 \pm 0.1$, $\varepsilon_2 = -0.25 \pm 0.005$, and $\varepsilon_3 = -4.0 \pm 0.5$. These values agree well with the constants we calculated from the third-order elastic moduli of synthetic fused silica, but differ significantly from those found for fused quartz (Herasil). These findings demonstrate the potential of the method for materials characterization with laser-generated high-amplitude SAW pulses and the determination of the nonlinear acoustic constants.

ACKNOWLEDGMENTS

We thank S. Zherebtsov for assistance in the construction of the setup. Support from NSF (Grants No. 9870143 and No. 9970241) is gratefully acknowledged.

[1] A. P. Mayer, Phys. Rep. **256**, 237 (1995).
[2] A. V. Nikolaev, Phys. Earth Planet. Inter. **50**, 1 (1988).
[3] Al. A. Kolomenskii, V. G. Mikhalevich, A. A. Maznev, and H. A. Schuessler, J. Appl. Phys. **84**, 2404 (1998).
[4] Al. A. Kolomenskii, A. M. Lomonosov, R. Kuschnereit, P. Hess, and V. E. Gusev, Phys. Rev. Lett. **79**, 1325 (1997).
[5] E. G. Lean, C. C. Tseng, and C. G. Powell, Appl. Phys. Lett. **16**, 32 (1970).
[6] A. J. Slobodnik, Jr., J. Acoust. Soc. Am. **48**, 203 (1970).
[7] A. Lomonosov, V. G. Mikhalevich, P. Hess, E. Yu. Knight, M. F. Hamilton, and E. A. Zabolotskaya, J. Acoust. Soc. Am. **105**, 2093 (1999).
[8] E. A. Zabolotskaya, J. Acoust. Soc. Am. **91**, 2569 (1992).
[9] V. E. Gusev, W. Lauriks, and J. Thoen, Phys. Rev. B **55**, 9344 (1997).
[10] Al. A. Kolomenskii and A. A. Maznev, Akust. Zh. **36**, 463 (1990) [Sov. Phys. Acoust. **36**, 258 (1990)].
[11] V. E. Gusev, W. Lauriks, and J. Thoen, J. Acoust. Soc. Am. **103**, 3203 (1998).
[12] R. T. Smith, R. Stern, and R. W. B. Stephens, J. Acoust. Soc. Am. **40**, 1002 (1966).
[13] W. T. Yost and M. A. Breazeale, J. Appl. Phys. **44**, 1909 (1973).
[14] E. H. Bogardus, J. Appl. Phys. **36**, 2504 (1965).
[15] Melles Griot, *Catalog* (Melles Griot Inc., Irvine, 1995/96), pp. 4 and 5; *The Properties of Optical Glass*, edited by H. Bach and N. Neuroth (Springer, New York, 1995).